# Tolerance Evaluation for Defocused Images to Optical Watermarking Technique

Yasunori Ishikawa, Kazutake Uehira, Member, IEEE, and Kazuhisa Yanaka, Member, IEEE

Abstract—In this paper, we describe a new aspect to evaluating the robustness of the optical watermarking technique, which is a unique technology that can add watermarked information to object image data taken with digital cameras without any specific extra hardware architecture. However, since this technology uses light with embedded watermarked information, which is irradiated onto object images, the condition of taking a picture with digital cameras may affect the accuracy with which embedded watermarked data can be detected. Images taken with digital cameras are usually defocused, which occurs under non-optimal conditions. We evaluated the defocusing in images against the accuracy with which optical watermarking could be detected. Defocusing in images can be expressed with convolution with a line-spread function (LSF). We used the value of full-width at half-maximum (FWHM) of a Gaussian function as the degree to which images were defocused, which could approximate LSF. We carried out experiments where the accuracies of detection were evaluated as we varied the degree to which images were defocused. The results from the experiments revealed that optical watermarking technology was extremely robust against defocusing in images.

Index Terms—Digital watermarking, optical watermarking, spatially modulated illumination, visible light communication.

### I. Introduction

ATERMARKING technology has spread widely around the globe due to the world-wide distribution of multimedia content through the various methods of networking [1]–[5], [9]. Intellectual Property rights, like copyrights or the photographic rights of content, should be strictly protected in these various situations. We proposed "optical watermarking" technology as one solution to this problem that uses illumination containing invisible watermarked information. When the illumination is projected onto real objects and the photographs are taken by digital cameras, the digital data on the photographs also contain invisible watermarked information. One of the unique features of this technology is that it can be used to embed invisible digital watermarking information into the image data of real objects with spatially modulated illumination. Therefore, this technology has different features from conventional digital watermarking technologies. When conventional digital watermarking technologies are used, images of objects with no copyright protection, such as pictures in

Manuscript received January 11, 2013; revised April 30, 2013; accepted September 22, 2013. Date of publication October 10, 2013; date of current version January 20, 2014.

The authors are with the Kanagawa Institute of Technology, Atsugi-shi, Kanagawa, Japan(e-mail: yasu@yit-pe.com; uehira@nw.kanagawa-it.ac.jp; yanaka@ic.kanagawa-it.ac.jp).

Digital Object Identifier 10.1109/JDT.2013.2285436

museums painted by famous artists, cannot be prevented from being illegally photographed. This is because that watermarked information has to be embedded into the image data before they are used in conventional watermarking technologies. Optical watermarking technology can offer a solution to resolve such difficult situations.

Tan *et al.* proposed a technique where a pattern was projected onto person's body with a projector and the embedded pattern could be detected from the printed image taken by a camera. They used the magnitude coefficients of a discrete Fourier transform (DFT) and the blue channel of the color image data embedded into the image pattern [7]. This technology may be used for security purpose in identifying people at passport control for example.

We proposed the use of orthogonal transforms such as a discrete cosine transform (DCT) and a Walsh-Hadamard transform (WHT) as a practical method of using optical watermarking technology to embed watermarked information into illumination [6], [8]. We also conducted various practical experiments in real-use environments. For example, we proposed a technique that was robust against geometrical distortions under practical shooting and reflectance conditions, where the conditions under which images of objects were taken were not optimal [10]. We also proposed optimizing of the pixel sizes of blocks in watermarked images, where the relation between the pixel sizes of blocks, accuracy of detection, and volume of content were evaluated [11]. However, if a practical environment is considered where illegal photographs are taken by digital cameras, the distance between the object to be photographed and the camera to be used may not be the optimal position when focusing is considered. We focused on evaluating the accuracy with which the optical watermarking in defocused images could be detected, which could be produced under such photographic conditions in this research. From the results of the experiments, we found optical watermarking technology was extremely strong in tolerance against defocusing.

## II. MATHEMATICAL EXPRESSION OF DEFOCUSED IMAGE DATA

The image data for a photographed object are expressed by convolution with the point spread function (PSF), which indicates the characteristics of the optical system used for the photography and the reflectance distribution of the object. Therefore, the defocused image data that are produced for an object with an optical system can be expressed by convolution with PSF that has characteristics of the optical system. Since PSF can be approximated with a Gaussian function, we used the full-width at half-maximum (FWHM) of a Gaussian function as characteristics that indicate the degree of defocusing image

data in the experiments. We measured the defocusing value in the experiments using the response of the density value by reading the image data of an isolated point one-dimensionally (horizontally). Therefore, a line-spread function (LSF) could be equivalently adapted to approximate a one-dimensional Gaussian function.

The one-dimensional Gaussian function is expressed by

$$f(x) = a \bullet \exp\left\{-\frac{(x-b)^2}{2c^2}\right\} \tag{1}$$

for some real constants a,b,c, and  $\exp$  means the exponential function of Euler's number (base of a natural logarithm):  $e\approx 2.71828$  [12], [13]. The FWHM of a one-dimensional "normalized Gaussian function", i.e., a one-dimensional Gaussian function whose surface area for the whole integration domain is one, is expressed by

$$w = 2\sqrt{2\ln 2}c\tag{2}$$

where w is equivalent to FWHM that indicates the horizontal width of the one-dimensional Gaussian function at half its maximum value, and  $\ln$  means a natural logarithm. When  $\ln 2 = 0.6931471$  is placed

$$\frac{1}{c^2} = \frac{5.5451768}{w^2} \tag{3}$$

the denominator in the exponential function in (1) is

$$\frac{1}{2c^2} = \frac{2.7725884}{w^2}. (4)$$

Therefore, a one-dimensional normalized Gaussian function is expressed by

$$h(x) = \sqrt{\frac{2.7725887}{\pi w^2}} \exp\left\{-\frac{2.7725887(x - x_0)^2}{w^2}\right\}$$
 (5)

where  $x_0$  is the central value of the Gaussian function. The convolution with normalized Gaussian function h(x) given in (5) to object image f(x) is expressed by

$$g(x) = \int_{-\infty}^{\infty} f(x')h(x - x')dx'. \tag{6}$$

We used a rectangular function that was 11 pixels in width and 24 pixels in height as an isolated point image as f(x) in (6) to maintain consistency with the data in the experiments. Furthermore, convolution was calculated with the one-dimensional Gaussian function with the w pixel(s) of the FWHM. The simulated waveforms for the response of the density value of defocused images were produced as the calculation results. Fig. 1 has the simulation waveforms for the response of the density value, where FWHM was set from one to 15 pixels (all odd pixels). We used these waveforms to identify the FWHM of the real response of the image we obtained for the isolated points.

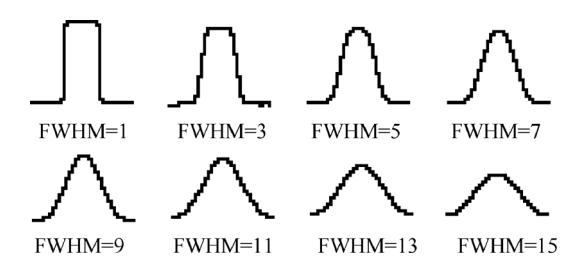


Fig. 1. Simulation waveforms for response of rectangular function (units of FWHM: pixels).

#### III. EXPERIMENTS

# A. Generation of Watermarking Information Using Orthogonal Transforms

We first produced watermarking information using orthogonal transforms in the experiments. The watermarked area was divided into numerous blocks and each had 8×8 pixels. The average brightness in every block was given as a DC component in the frequency space of an orthogonal transform. Therefore, the average brightness of the entire area for watermarking was determined by the DC component, which was the brightness of illumination to be projected onto objects. Also, the highest frequency component (HC) in frequency space both horizontally and vertically was used to embed watermarking information. That is, the HC was used to express the one-bit binary information for watermarking. The phase of HC was used in the experiments to express binary data. If the phase of HC in a block was positive, this was assumed to be expressed as "logical 1", and if the phase was negative, this was assumed to be expressed as "logical 0". When 2D inverse DCT (i-DCT) is used to generate the watermarked image, which is expressed by

$$f_{i,j}(x,y) = \sum_{u}^{N-1} \sum_{v}^{N-1} C(u)C(v)F_{i,j}(u,v)$$

$$\bullet \cos\left\{\frac{(2x+1)u\pi}{2N}\right\} \cos\left\{\frac{(2y+1)v\pi}{2N}\right\}$$
(7)

where  $f_{i,j}(x,y)$  are the watermarked image data for the pixel (x,y) of block (i,j) in real space,  $F_{i,j}(u,v)$  are the data for component (u,v) of block (i,j) in frequency space, and N is the number of pixels in the block in the x- and y-directions. Here, C(u) and C(v) are given as

$$C(u) = \begin{cases} 1 & (u = 0) \\ \sqrt{2} & (u \neq 0) \end{cases}, \quad C(v) = \begin{cases} 1 & (v = 0) \\ \sqrt{2} & (v \neq 0) \end{cases}$$

2D inverse WHT (i-WHT) is used to produce the watermarked image, which is expressed by

$$f_{i,j}(x,y) = \frac{1}{N} \sum_{i=1}^{N-1} \sum_{v=1}^{N-1} F_{i,j}(u,v) w h(x,u) w h(v,y)$$
(8)

where wh(i,j) denotes the  $N\times N$  Walsh-Hadamard matrix component [8]. Because the frequency components of the object image itself were usually lower than HC, the embedded information for watermarking could be easily separated from the object image. The N was set to eight in the experiments.

When the watermarked information was detected from the image data we obtained, forward orthogonal transforms were used. When using 2D forward DCT, which is expressed by

$$F_{i,j}(u,v) = \frac{C(u)C(v)}{N \times N} \sum_{x}^{N-1} \sum_{y}^{N-1} f_{i,j}(x,y)$$

$$\bullet \cos \left\{ \frac{(2x+1)u\pi}{2N} \right\} \cos \left\{ \frac{(2y+1)v\pi}{2N} \right\}$$
(9)

and when using 2D WHT, which is expressed by

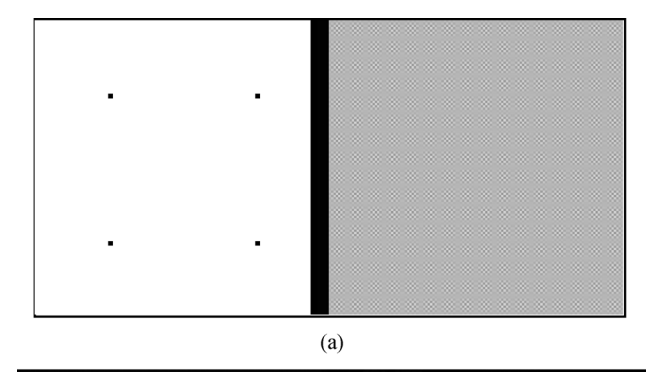
$$F_{i,j}(u,v) = \frac{1}{N} \sum_{x}^{N-1} \sum_{y}^{N-1} f_{i,j}(x,y) w h(u,x) w h(y,v)$$
 (10)

C(u), C(v), and wh(i, j) are the same as those in (7) and (8). The accuracy with which the embedded data were read out was evaluated by checking the sign of the  $F_{i,j}(N-1,N-1)$  components for all blocks in (9) and (10).

We used two methods of embedding the data in the experiments. The first method was the "one-block method", which involved embedding one-bit data into one block. The second method was the "majority method", which involved embedding the same one-bit data into three blocks sufficiently separated from one another. The readout data were determined by majority decision using these three blocks. The latter method might have improved the accuracy with which the embedded data were read out.

# B. Producing the Experimental Image Data and the Conditions of the Experiments

We next generated image data that were projected onto the object. Two sets of image data were horizontally fixed, which were the watermarked images produced with orthogonal transforms on the right and the image on which only four  $2\times 2$ -pixel isolated points had been drawn on the left, where DCT and WHT were used as the orthogonal transforms previously mentioned. The watermarked images were produced as blocks that were embedded with binary watermarked information of "0" and "1", and were alternately placed in a checkerboard pattern. There were  $128 \times 128$  pixels in the watermarked images, where  $16 \times 16$  blocks of  $8 \times 8$  pixels were contained, and there were  $128 \times 120$  pixels in the images that contained the isolated point. Therefore, there was 8-pixels crevice between the left side and the right side of the generated image data. Fig. 2(a) shows the generated image data that were projected onto the object with the projector. The object was a plain sheet of paper on the wall that had two rectangular areas, which also had white paper stuck on the left and printed standard image data on the right. Each of them was A4 size with portrait orientation. An SCID N2 image was used as standard image data [14]. Further, the generated image data were irradiated onto the object on the wall with a projector, where the watermarked image data were projected



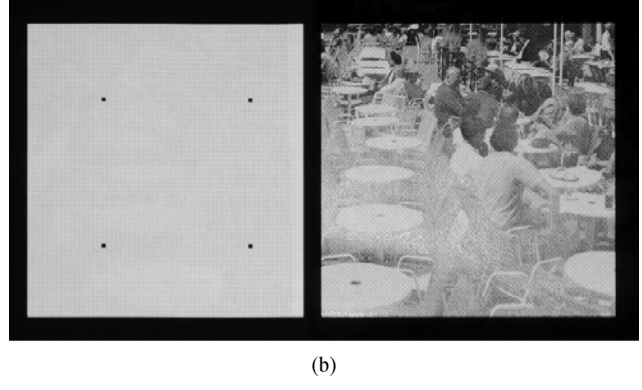


Fig. 2. (a). Generated image data to be projected onto objects—Left: Isolated points—Right: Watermarked image (DCT, HC=15). (b). Image obtained from experiments—Left: Isolated points area to measure defocusing—Right: Watermarked image area (DCT, HC=15).

onto the printed standard image and the image data with isolated points were projected onto white paper. Using these experimental environments, we intended to measure the defocusing value of the images and evaluate the accuracy with which embedded watermarked information had been detected from the defocused image data that had the measured defocusing value.

We then took a picture of the object that was projected with the generated image data with a digital camera. Fig. 2(b) has the image obtained from the experiments where the left side is the isolated point area we used to measure defocusing in the image and the right side is the watermarked image of the printed SCID N2 image. A Digital Light Processing (DLP) projector with a resolution of 800×600 pixels was used in the environment for the experiments to irradiate the generated image onto the object and a digital camera with a resolution of  $4288 \times 2848$ pixels was used to take a picture of the object. The distance from the projector to the object image plane was set to about 1.1 m, and the distance between the lens surface of the digital camera and the object plane was set to about 1.3 m. A zoom lens was mounted onto the digital camera and a 70-mm focal length was used. The actual size of the irradiated watermarked image area on the printed image was about  $105 \times 105$  mm, and the area of the image data we obtained with the digital camera was about  $800 \times 800$  pixels. We acquired image data for the isolated points and the watermarked image by fluctuating the focal length slightly to evaluate what influence defocusing the image had on the accuracy with which the embedded watermarked information could be detected.

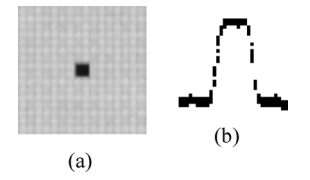


Fig. 3. Isolated point image and waveform of density (FWHM = 3). (a) Isolated point image. (b) Waveform of density.

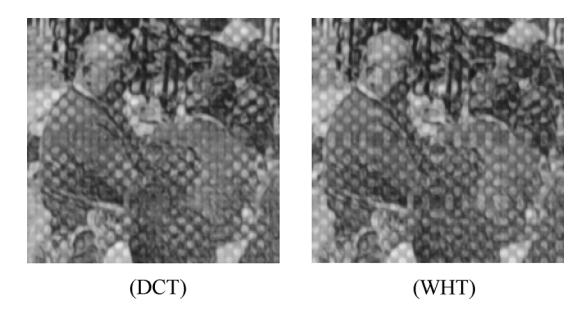


Fig. 4. Part of magnified image of watermarked area (FWHM = 3, DC = 150, HC = 15).

### C. Processing for Obtained Image Data

We will next explain the three-part process we used for the image data we acquired.

The first part of the process was executed on pixels in the area with isolated points. Referring to the "isolated point image" in Fig. 3(a) for example, the value of the pixels was read out horizontally on an approximately centered line on the isolated points to measure the density of the pixels. From this process, we acquired the "waveforms of density" in Fig. 3(b) for example, which were actually generated with the pixels of isolated point images having the same focal length.

The second part of the process was executed on watermarked images. A rectangle in the watermarked area was clipped out from the acquired image data and the resolution of the clipped rectangle was then transformed to just  $256 \times 256$  pixels, and divided into  $16 \times 16$  blocks each of which had  $8 \times 8$  pixels. Then a forward orthogonal transform (DCT or WHT) corresponding to the method with which watermarking was produced was applied to all blocks in the clipped out area. Embedded binary information was read out by checking the HC value of all blocks, i.e.,  $F_{i,j}(7,7)$  components for all blocks in frequency space, and the rate at which blocks were correctly read out was determined. Blocks embedded with "1" and "0" were alternately placed in checkerboard fashion in the watermarked area in the experiments. The accuracy of detection was measured from these results.

The third part of the process was to estimate LSF FWHM. LSF FWHM could be identified by comparing the waveforms of density that were obtained with the first process with the simulation waveforms for the response of the density value. For example, the waveform of density in Fig. 3(b) was compared with the simulation waveforms in Fig. 1. Identification was undertaken by comparing the pixel width at a height of 23 pixels from the base of the wave to obtain more detail. However, the maximum height of the waveform was used for identification

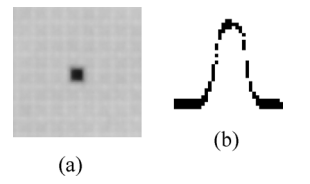


Fig. 5. Isolated point image and waveform of density (FWHM = 5). (a) Isolated point image. (b) Waveform of density.

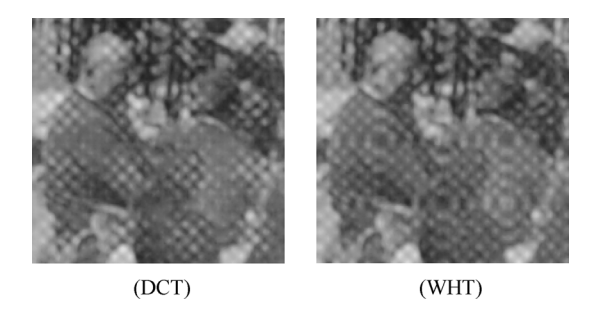


Fig. 6. Part of magnified image of watermarked area (FWHM = 5, DC = 150, HC = 15).

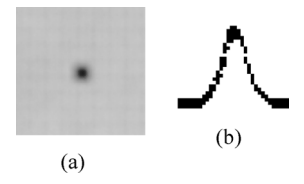


Fig. 7. Isolated point image and waveform of density (FWHM = 7). (a) Isolated point image. (b) Waveform of density.

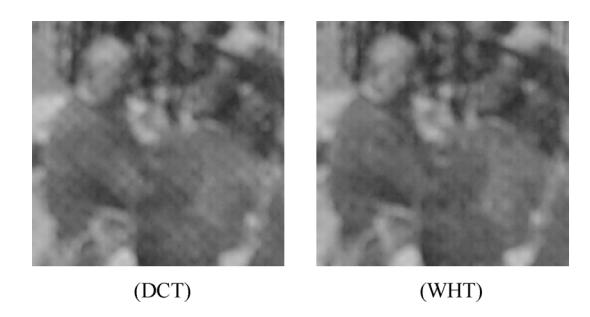


Fig. 8. Part of magnified image of watermarked area (FWHM = 7, DC = 150, HC = 15).

when the height from the base was under 23 pixels. The defocusing of the watermarked image data was estimated to be the same as the corresponding FWHM.

### IV. RESULTS AND DISCUSSION

Figs. 3 and 4; 5 and 6; 7 and 8; 9 and 10; and 11 and 12 have the magnified images of the isolated points, the waveforms for density values of the isolated points, and the watermarked areas (DCT and WHT) at FWHM = 3, 5, 7, 9, and 11, respectively. FWHM was identified with the process described in the previous section. We would summarize from Figs. 3–12 that the degree in defocusing of images for the isolated points and the watermarked images could be observed in terms of FWHM. Figs. 13 – 16 also plot the accuracies of detection as the values of FWHM are experimental parameters, where HC = 5, 10, and

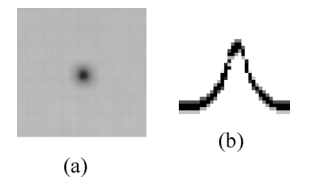


Fig. 9. Isolated point image and waveform of density (FWHM = 9). (a) Isolated point image. (b) Waveform of density.

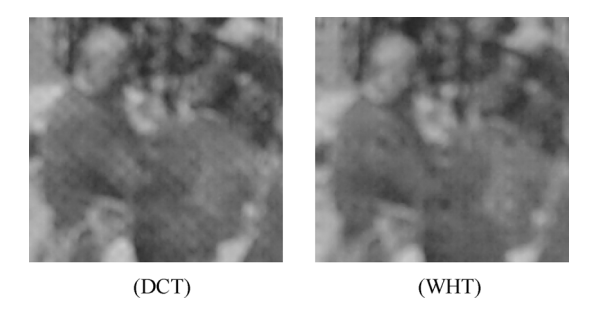


Fig. 10. Part of magnified image of watermarked area (FWHM = 9, DC = 150, HC = 15).

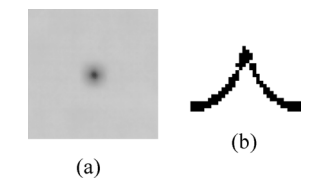


Fig. 11. Isolated point image and waveform of density (FWHM = 11). (a) Isolated point image. (b) Waveform of density.

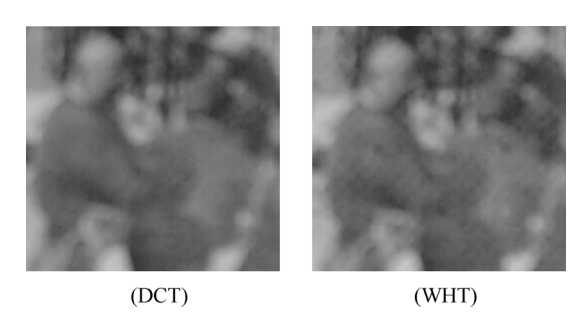


Fig. 12. Part of magnified image of watermarked area (FWHM = 11, DC = 150, HC = 15).

15 were used as the strength of embedded optical watermarking. The one-block and majority methods were used to embed watermarking to enable the accuracies of detection with DCT and WHT to be evaluated. Here, the distance between the blocks in the majority method that had the same information was set to five in the experiments.

When the actual images of the isolated points and the watermarked images are observed in Figs. 3–12, defocusing of images is not great (i.e., the images are almost in focus) at FWHM = 3. However, the degree to which defocusing increases can be clearly identified, as the value of FWHM increases. Moreover, when the watermarked area images are observed in detail, although the patterns for DCT and WHT can

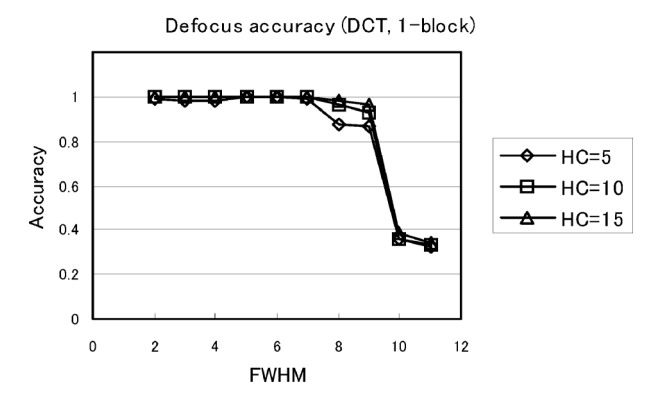


Fig. 13. Accuracy under defocusing conditions (DCT, 1-block method).

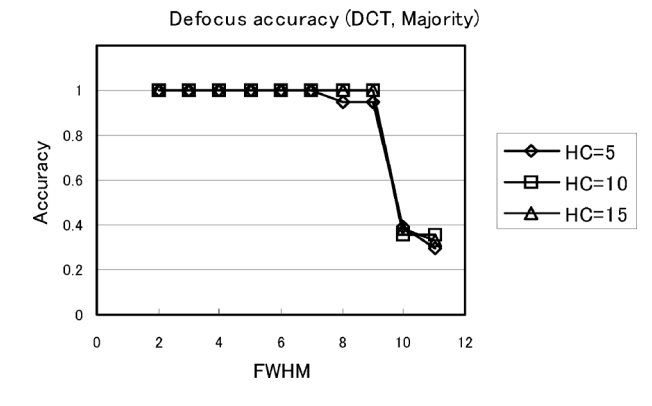


Fig. 14. Accuracy under defocusing conditions (DCT, Majority method).

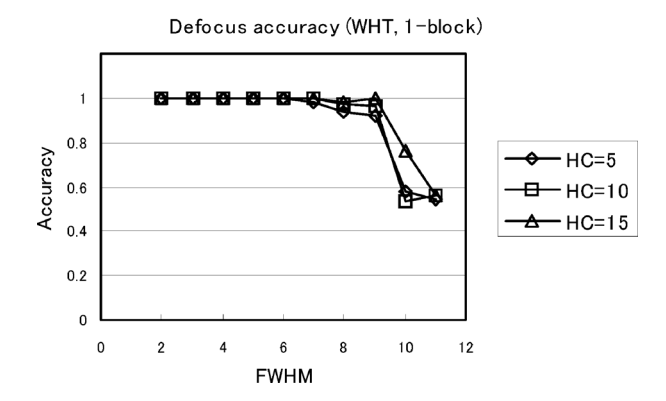


Fig. 15. Accuracy under defocusing conditions (WHT, 1-block method).

be obviously recognized at FWHM = 5 or less (because embedding is rather strong at HC = 15), these patterns are difficult to observe at FWHM = 7 or more. The patterns are almost non-recognizable especially at FWHM = 11. This appeared noticeably in the results obtained from evaluating the accuracy of detection in Figs. 13–16. That is, when FWHM was nine pixels or less, the accuracy of detection was not less than 94% in total according to the majority method. However, when FWHM was 10 pixels or more, the accuracy decreased rapidly. Particularly when FWHM was seven pixels or less in defocused images, an accuracy of detection of 100% was obtained for all HC values, according to the majority method using DCT and WHT. Moreover, the accuracy was near 100% when the one-block method was used under the same conditions as

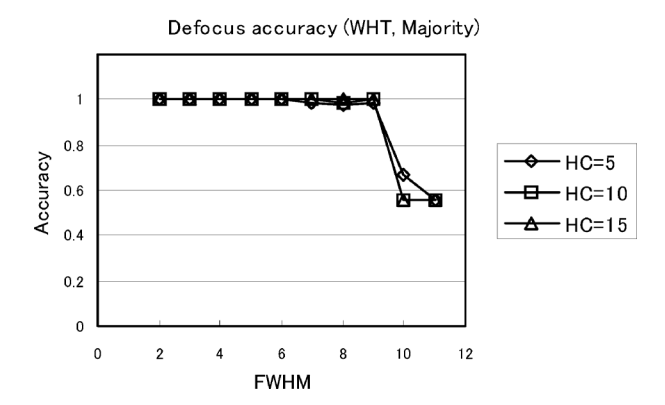


Fig. 16. Accuracy under defocusing conditions (WHT, Majority method).

those for the majority method. From Figs. 7-12, we can see intense defocusing on the images of isolated points and watermarked areas under the conditions of FWHM = 7, 9 and 11, respectively. However, the experimental results revealed that almost 100% accuracy in detection could be obtained under such defocusing intensity using the majority method for embedded watermarked information (see Figs. 14 and 16). Also, an accuracy of detection of more than 90% could be obtained when the one-block method was used.

These experimental results depend on the characteristics of the specific optical system used in the experiments. However, judging from observations of the defocused images (isolated point images and watermarked area images) in the experimental results, we found that optical watermarking technology has very high tolerance to defocused images.

### V. CONCLUSION

We conclude the following:

- 1) We evaluated degradation in the accuracy of detection that arose from defocusing in images, where the FWHM of a one-dimensional Gaussian function, which approximated LSF, was used to measure the degree of defocusing in images. We measured the FWHM of isolated points and evaluated the accuracy with which the watermarked images could be detected when the focal length of the digital camera was changed.
- 2) When defocusing had occurred in images whose FWHM for the normalized one-dimensional Gaussian function was nine pixels or less, we found that the accuracy of detection was close to 100% under conditions beyond HC=5 when the majority method was used.
- 3) Sufficiently high accuracy of detection could be acquired, even when intense defocusing had occurred in images at nine pixels of FWHM or less, by observing pictures taken with a digital camera and then comparing with the images actually defocused with increased FWHM values.

Optical watermarking technology can be used to superimpose invisible information on the images of objects taken, as a photograph of objects irradiated with optical watermarked information, with digital cameras or smart phones. Consequently, this technology can be applied to prevent illegal contents, i.e., photographs illegally taken at art museums, movie theaters, or concerts on stages. It can also be used as an explanatory tool for exhibits at museums and for goods at shopping centers. However, we need to evaluate its robustness against various degrees of disturbances in detecting watermarked information like that in other digital watermarking technologies. For example, its tolerance to geometric distortion, image data compression such as that in JPEG, and various image processes needed to be evaluated and resolved. Furthermore, its tolerance to defocusing of images derived from the characteristics of the optical system when photographs of objects are taken under non-optimal conditions needed to be evaluated as a subject that is unique to optical watermarking technology.

From the results of the experiments, we concluded that optical watermarking has strong tolerance to defocusing in images.

#### REFERENCES

- [1] I. J. Cox, J. Kilian, F. T. Leighton, and T. Shamoon, "Secure spread spectrum watermarking for multimedia," *IEEE Trans. Image Process.*, vol. 6, no. 12, pp. 1673–1687, Dec. 1997.
- [2] M. Hartung and M. Kutter, "Multimedia watermarking techniques," Proc IEEE, vol. 87, no. 7, pp. 1079–1107, Jul. 1999.
- [3] J. Haitsma and T. Kalker, "A watermarking scheme for digital cinema," in *ICIP2001*, 2001, vol. 2, pp. 487–489.
- [4] T. Mizumoto and K. Matsui, "Robustness investigation of DCT digital watermark for printing and scanning," *Trans. IEICE (A)*, vol. J85-A, no. 4, pp. 451–459, 2002.
- [5] Z. Liu, "New trends and challenges in digital watermarking technology: Application for printed materials," in *Multimedia Watermarking Techniques and Applications*, B. Furht and D. Kirovski, Eds. : Auerbach Publications, 2006, pp. 289–305.
- [6] K. Uehira and M. Suzuki, "Digital watermarking technique using brightness-modulated light," in *Proc. ICME2008*, 2008, pp. 257–260.
- [7] Y. Tan, H. Liu, S. Huang, B. Sheng, and Z. Pan, "An optical water-marking solution for color personal identification pictures," in *Proc. SPIE2009*, 2009, vol. 7512, p. 75120A.
- [8] Y. Ishikawa, K. Uehira, and K. Yanaka, "Practical evaluation of Illumination watermarking technique using orthogonal transforms," *J. Display Technol.*, vol. 6, no. 9, pp. 351–358, 2010.
- [9] T. Yamada, S. Gohshi, and I. Echizen, "Re-shooting prevention based on difference between sensory perceptions of humans and devices," in *Proc. ICIP 2010*, Hong Kong, Sep. 2010.
- [10] Y. Ishikawa, K. Uehira, and K. Yanaka, "Optical watermarking technique robust to geometrical distortion in image," in *Proc. ISSPIT2010*, 2010, pp. 67–72.
- [11] Y. Ishikawa, K. Uehira, and K. Yanaka, "Robust optical watermarking technique by optimizing the size of pixel blocks of orthogonal transforme," in *Proc. IAS2011*, Oct. 2011.
- [12] A. Rosenfeld and A. C. Kak, *Digital Picture Processing*. New York: Academic Press, 1976.
- [13] [Online]. Available: http://en.wikipedia.org/wiki/Gaussian\_function Accessed: Dec. 30, 2012
- [14] Graphic Technology Prepress Digital Data Exchange CMYK Standard Colour Image Data (CMYK/SCID), ISO 12640, 1997.

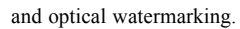


Yasunori Ishikawa received the B.S. degree in measurement and instrumentation engineering from the University of Tokyo, Japan, in 1977, and the Ph.D. degree in information engineering from Kanagawa Institute of Technology, Japan, in 2011. He worked for Fuji Electric Corporation and Ricoh Corporation from 1977 to 2001, where his work involved the research and development of embedded systems for consumer products, image processing and communication products, and research on image compression. Since 2001, he has been the president

of YIT Consulting Corporation, Japan, offering technical consulting and technology transfer in his fields of expertise.



Kazutake Uehira received the B.S. and M.S. degrees in electronics in 1979 and 1981, respectively, and the Ph.D. degree in 1994, all from the University of Osaka Prefecture in Osaka, Japan. He joined NTT Electrical Communication Laboratories in Tokyo, Japan, in 1981. Since then, he has been engaged in the research and development of image acquisition technologies, display systems, and high-reality video communication systems. In 2001, he joined Kanagawa Institute of Technology as a professor and is currently engaged in research on 3-D displays





Kazuhisa Yanaka received the B.S., M.S., and D.E. degrees from the University of Tokyo in 1977, 1979, and 1982, respectively. He joined NTT Electrical Communication Laboratories in Tokyo, Japan, in 1982. He joined Kanagawa Institute of Technology in 1997, where he is currently a professor. For more than 30 years, he has been researching various aspects of images such as image processing, image communication, image input/output systems, and optical watermarking.